

# A Tree-structured LoRa Network for Energy Efficiency

Yas Hosseini Tehrani, Arash Amini, *Senior Member, IEEE*, and Seyed Mojtaba Atarodi, *Senior Member, IEEE*

**Abstract**—The LoRa technology is considered as one of the most potential solutions for IoT in the near future. The existing LoRa networks are based on the star topology. In this paper, a tree network adopted for the LoRa technology and a communication protocol are proposed to mitigate the energy consumption constraints. In the proposed network, the nodes are self-configured based on the LoRa physical link behavior and can act as relays to propagate data from other nodes. The analysis, design, and evaluation of the proposed architecture for large scale LoRa networks are presented in detail. With analytical studies, the energy consumption of the star and tree LoRa networks are compared. The presented analytical results can provide developers with effective guidelines for scalable design and optimization of LoRa networks. Further, the results are verified using simulation and experimental tests. Both simulation and experimental results confirm that the presented method improves the energy consumption of the entire IoT network significantly. As a result, the presented tree network can be deployed in various applications.

**Index Terms**—Energy efficient, LoRa, Optimization, Star topology, Tree topology.

## I. INTRODUCTION

**T**HE Internet of things (IoT) is an emerging technology, encompassing wide aspects of applications. It provides intelligent connections between objects, devices, and living creatures. The IoT applications require low-cost, low-energy, reliable, robust, secure, and scalable networks. The IoT devices are mostly powered by limited energy sources like batteries. Therefore, optimizing their power consumption is necessary. There are many technologies such as NB-IoT, Sigfox, ZigBee, LoRa, and Bluetooth that enable IoT deployment [1], [2], [3]. LoRa is one of the promising low-power wide area network (LPWAN) technologies promoted by the LoRa alliance. It has attracted a great deal of interest in the field of IoT. It provides a flexible, easily configurable, and inexpensive network among IoT nodes. The LoRa modulation is based on the chirp spreading spectrum (CSS). In this technology, the signal is spread over a wide frequency band. The slope of the chirps is determined by the spreading factor (SF) [4]. In this technology, there is a tradeoff between the data rate and the sensitivity, which can be adjusted by setting the SF value. Besides, LoRa signals with different spreading factor values are quasi-orthogonal to each other [5], [6]. The typical LoRa topology is based on a star network [7]. It is a single-hop network based on the ALOHA protocol in which nodes communicate whenever its needed. Many strategies are proposed for the performance

enhancement of the LoRa network. The Adaptive Data Rate (ADR) method is introduced by LoRa alliance for data rate, air time, and energy consumption optimization. This method has drawbacks in dense and high varying wireless environments [8]. The LoRa technology is expected to offer energy-efficient networks with a high number of low-power devices, distributed in large geographical areas [9]. The tree-based Lora network proposed in this paper improves the energy consumption of the network. Also, it extends the network coverage and increases the communication reliability. To investigate and validate the performance of the proposed algorithms, the tree and star LoRa networks are modeled, simulated and implemented. The analytical and simulation results reveal that the energy consumption of the LoRa network with 100 nodes in the tree topology is around 79% and 84% below that of the star topology, respectively. The efficiency of the tree network degrades by decreasing the number of the nodes. For instance, The improvement percentage of energy consumption of the tree network with 35 nodes obtained from analytical, simulation, and experimental results is around 58%, 69%, and 46%, respectively.

This paper is organized as follows. Some of the recent studies on energy efficiency of wireless sensor networks (WSNs) are reviewed in Section II. Section III introduces the LoRa basics in detail. Also, some related works in LoRa WSN are presented. Section IV presents the proposed energy reduction algorithms for the star and tree-based LoRa network. The analytical studies of the proposed algorithms are provided in Section V. In the next section, the simulation results are presented. Section VII focuses on the implementation, experimental results and key features of the proposed algorithms. Finally, the conclusions are given in Section VIII.

## II. ENERGY EFFICIENCY IN WSNs

The energy consumption is one of the main concerns of WSNs; it is desirable to keep the overall energy consumption as low as possible. The structure of the network varies based on the communication technology, number of the nodes, environment, the application requirements, and the available resources. WSN typologies are generally divided into the two main categories of centralized and distributed networks. In a centralized network, the central unit has multiple options to improve the energy efficiency. These options include data reduction, protocol overhead reduction, energy-efficient routing, duty cycling, and topology control [10]; the literature in each of these options is quite rich. In hierarchical protocols such as HEED [11] and EECHA [12], nodes are clustered

The authors are with the Electrical Engineering department, Sharif university of technology, Tehran, Iran. Email: yas.hosseini@ee.sharif.edu, aamini@sharif.edu, atarodi@sharif.edu (corresponding author).

with each cluster having a head. The communication primarily takes place within the cluster and the head is responsible for all intra-cluster communications. To balance the load on clusters, chains of nodes are formed after selecting the optimal cluster head. In [13], an unequal clustering with a multi-path algorithm and multi-hop communication is deployed. This approach, however, suffers from increased processing overhead and data redundancy. For IoT applications, new routing protocols such as AODV [14] are proposed; unfortunately, metrics such as load balance and energy efficiency are not emphasized much in these protocols. Among other recent routing strategies one can name the optimized link state routing protocol (OLSR) [15], the destination-sequenced distance vector routing protocol (DSDV) [16], the dynamic source routing (DSR) [17], and the zone routing protocol (ZRP) [18]. To evaluate the energy consumption of each protocol, the specific application, the physical layer technology and the available resources shall be taken into account. In terms of energy loss, the hierarchical network strategies are typically superior than the flat strategy (non-hierarchical) because of the latency factor. However, the flat strategy has the performance advantage because of the lower level of overhead requirements.

In the next section, we shall address the issue of energy consumption in a LoRa network.

### III. LORA BASICS

#### A. LoRa Modulation

LoRa is one of the most successful LPWAN technologies which can operate in sub-GHz frequency bands [19]. The long range, high robustness, multipath resistance, and low power communication are the key features. The communication performance of LoRa transceiver is achieved by properly setting the configurations, including the bandwidth, the spreading factor, the coding rate, and the transmission power.

1) *Bandwidth*: The LoRa transceiver (SX1276) has programmable bandwidth in the range of 7.8 kHz to 500 kHz. However, according to LoRaWAN specifications, typical LoRa networks mainly use bandwidth settings of 500 kHz, 250 kHz, and 125 kHz. Moreover, a temperature compensated oscillator is required for bandwidths below 62.5 kHz [20]. Therefore, only typical bandwidth settings (500 kHz, 250 kHz and 125 kHz) are considered in this study. The sensitivity and data rate of LoRa links are inversely and directly related to the bandwidth, respectively [21].

2) *Spreading Factor*: The ratio between the symbol rate and chip rate is called the spreading factor in LoRa terminology. The higher signal to noise, and thus higher communication range and higher sensitivity are achieved by increasing the value of spreading factor. Note that different nodes in the same LoRa network can use different spreading factors, as links with different spreading factors are quasi-orthogonal and the resulting interference is mainly tolerable [22]. While the spreading factor can take values from 6 to 12, the case of  $SF = 6$  is rarely used in typical LoRa networks ( $SF = 7$  to  $SF = 12$  are selected according to LoRaWAN specifications). The symbol rate  $R_S$  can be obtained from (1).

$$R_S = \frac{BW}{2^{SF}}, \quad (1)$$

where  $BW$  and  $SF$  are the bandwidth and the spreading factor, respectively [23].

3) *Coding Rate*: The LoRa technology supports forward error correction to provide protection against bursts of interference. A higher protection level is achieved by a higher coding rate. The coding rate value can be tuned between 1 and 4. The bit-rate  $BR$  of LoRa is computed as:

$$BR = SF \cdot \frac{4}{4+CR} \cdot \frac{BW}{2^{SF}}, \quad (2)$$

where  $CR$  is the value of the coding rate [24].

4) *Transmission power*: The LoRa transmission power can be adjusted from  $-4$  dBm to  $+20$  dBm. Both the power consumption and the communication range are increased by increasing the transmission power. It should be noted that, the transmission powers above  $+17$  dBm shall be checked with regulatory constraints [21].

#### B. LoRaWAN network topology

The LoRaWAN network consists of nodes, gateways, and a network server. The nodes are connected to the gateways using the ALOHA protocol as a medium access mechanism. The gateways are linked to a network server via an IP protocol. The gateways are more expensive than the nodes because they must be able to receive messages from multiple channels simultaneously which may have different configurations. The network server is responsible for collecting and decoding the packets sent by the nodes. It can control the network by sending back the appropriate packets to the nodes [25].

Three different classes of nodes named as A, B, and C are defined in LoRaWAN specification. In class A, a node starts an up-link transmission followed by two short down-link receive windows. The nodes of class B have periodic receive windows at scheduled times. The class C nodes have continuous open receive windows after transmitting a message to the gateways [26].

#### C. LoRa physical frame format

The structure of LoRa physical frame packet format which is defined by LoRaWAN is initiated by a preamble followed by a PHY header and an optional header. The preamble begins with a sequence of up-chirps. The synchronization word is determined by the last two up-chirps. The size of the payload, the code rate of the rest of the frame, and the presentation of the CRC for the payload is determined by the header. Next, the payload and optional CRC are sent [21]. The number of symbols for transmitting the payload  $n_{pl}$  is determined by (3). The total size of the packet in symbols  $n_{packet}$  is computed by adding  $n_{pl}$  to the number of preamble symbols  $n_{pm}$  [21]:

$$n_{pl} = 8 + \max\left(0, \left\lceil \frac{(8PL - 4SF + 28 + 16CRC - 20IH)}{4(SF - 2DE)} \right\rceil (CR + 4) \right), \quad (3)$$

$$n_{packet} = n_{pl} + n_{pm}, \quad (4)$$

where  $PL$  is the number of payload bytes.  $IH = 0$  when the header is enabled and it is equal to 1 when no header is present.  $DE$  is 1 if the data rate optimization is activated, otherwise it is equal to 0 [21].

#### D. Path Loss model

The communication range depends on the path loss, transmission power, and the receiver sensitivity. Obtaining a comprehensive path loss model is a great challenge, since it is highly dependent on the temperature, the environment, and weather conditions. In this study, the common log-distance path loss model described in (5) is adopted [20], [27], [28]:

$$L_{pl} = \overline{L_{pl}}(d_0) + 10\gamma \log_{10} \left( \frac{d}{d_0} \right) + X_\sigma \text{ [dB]}, \quad (5)$$

where  $d_0$  is the reference distance,  $\overline{L_{pl}}(d_0)$  is the mean path loss at reference distance,  $\gamma$  is the path loss exponent, and  $X_\sigma$  is a normal (Gaussian) random variable with zero mean, reflecting the attenuation (in decibel) caused by flat fading [29]. If we only consider  $X_\sigma$  (slow fading or shadowing), the path-loss follows a normal distribution with variance  $\sigma^2$  which results in a log-normal distribution of the received power. For fast fading and multi-path propagation, the received power is modeled by a Rayleigh distribution or Ricean random variable [30]. If the received power at the receiver side exceeds the threshold of the receiver sensitivity, then the data transfer is counted as successful. In this study, we measure the sensitivity of the receiver and path loss parameters in an experimental setup. For this purpose, we establish a link between two LoRa transceivers by using one of them as a transmitter and the other as a receiver. The transmitter sequentially sends packets with all feasible choices of the bandwidth, spreading factors, and transmission power. The sensitivity of LoRa receiver is then, measured as the minimum RSSI value at the receiver side. Next, we find the difference between the transmitted and received powers to estimate the path loss parameters  $d_0$ ,  $\overline{L_{pl}}(d_0)$ ,  $\gamma$ , and  $\sigma$  via curve fitting. To ensure about the validity of the estimated values, the above test is repeated multiple times using different distances between the transmitter and the receiver.

#### E. Related works

The multi-hop communication is a known technique, and is even applied to the LoRa network. Here, we review some of the recent multi-hop communication studies for LoRa network.

The RPL-based multi-hop LoRa network is presented as a solution for lowering the probability of network interference and achieving the optimal SF for each communication link with constant frequency channel and bandwidth settings [31]. The packet delivery ratio of the network for a test setup of four LoRa transceivers is measured. The use of concurrent transmission (CT) multi-hop protocol in LoRa, called CT-LoRa, allows multiple nodes to transmit the same packets simultaneously; the transmitted packets are delayed by a randomly generated time offset. Simulation results indicate that CT-LoRa can improve the packet delivery ratio from 51% to 77% in a network with four LoRa transceivers [32]. Another variant called LoRaBlink employs a time-slotted channel access MAC protocol. The time synchronization is performed by beacons and each time frame contains 2 slots: one reserved for the information about the hop distance and the other for the actual data. The successful packet delivery ratio of this method is measured around 80% [33]. Moreover, a mesh network is

adopted to decrease the number of required base stations [34]. In this setup, three strategies are considered for the LoRa nodes after receiving a packet: if the LoRa node is final destination of the packet, then, it processes the packet; if the LoRa node is within the routing path of the packet, then, the node acts as a relay; if neither of the two previous conditions hold, the LoRa node ignores the packet. A simulated experiment with 19 LoRa transceivers reveals that the mesh topology improves the packet delivery ratio of the network compared to the star topology. Moreover, the hybrid LoRa mesh/LoRaWAN network is developed to improve the communication range in shadow areas when a regular LoRaWAN node is not reachable [35]. In another study, the transmission power and the packet delivery rate of the nodes are improved by deploying a two-hop network compared to the standard single-hop network [36].

## IV. PROPOSED ENERGY REDUCTION ALGORITHMS

The LoRa network is mainly deployed in areas with moderate to high density of static or semi-static sensors that transmit low-rate data. Besides, the delay is mostly tolerable in such networks. However, the energy consumption is a critical issue that might restrict the implementation of LoRa in many scenarios. To the best of our knowledge, optimizing the energy consumption without modifying the physical layer of the LoRa protocol is not studied in the past. We should highlight that the routing strategy in multi-hop LoRa communication is greatly influenced by the objective function; in particular, maximizing the throughput (reducing network interference, packet loss, etc) or minimizing the number of required base stations does not necessary minimize the energy consumption.

In this paper, we devise a routing scheme by taking into account the specificities of a typical LoRa WSN:

- Multiple nodes can send their data to a single node; the latter node shall wait to receive all the data before starting to transmit anything. This might increase the delay in the network. However, it is not an issue in LoRa WSN.
- The sensors are mainly static; therefore, the routing scheme is not required to be evaluated (or updated) continuously (constrained by power budget). In other words, the routing scheme is mainly a preprocessing step here which could be optimized.
- The number of sensors is large enough that a probabilistic model can fairly predict the average energy consumption of the network (no need for checking the worst-case scenarios).
- The energy consumption is the main objective. As a result, a node is not allowed to use other nodes located further away from the base station as relay (which might have channels with smaller overall delay).

#### A. Star topology

In the star topology, each node communicates with the base station independently. The range of the communication is limited to one hop and it is defined by a transmission range of a single node. In this study,  $N$  nodes are placed randomly around

a base station. The nodes are configured to reduce network power consumption. The settings of each node are determined by its distance to the base station. The proposed algorithm for minimizing the energy consumption of each node is as follows:

- 1) The path loss is calculated using (5), by knowing the distance of the node from the base station.
- 2) The energy consumption is calculated using (6) for all acceptable settings of the bandwidths, spreading factors, and transmission powers, which applies to the condition described in (7) and (8):

$$E_{TX} = P_{TX} \times t_{TX}, \quad (6)$$

$$P_{RX} = P_{TX} - L_{pl}(d), \quad (7)$$

$$P_{RX} > \text{sensitivity}_{RX}, \quad (8)$$

where  $E_{TX}$  is the transmission energy,  $P_{TX}$  is the transmission power,  $t_{TX}$  is the transmission time,  $P_{RX}$  is the reception power, and  $L_{pl}(d)$  is the path loss at distance  $d$ . The LoRa receiver sensitivity depends on the selected bandwidth and spreading factor. Increasing the spreading factor increases the receiver sensitivity, whereas increasing the bandwidth decreases LoRa receiver sensitivity [21].

- 3) The bandwidth, spreading factor, and transmission power of each node is set by finding the combination that minimizes  $E_{TX}$ .

Therefore, by applying the proposed algorithm, the setting of each node is determined independently. As a result, the energy consumption of the network will be reduced compared to the conventional star topologies such as ADR method.

### B. Tree topology

In the tree topology, the nodes can act as relays to propagate the data from nodes farther from the base station in a hierarchy. The highest level of the hierarchy consists of the nodes furthest away from the base station. These nodes shall be connected to the nodes in their communication range that are closer to the base station. The same strategy is applied to the nodes in the next hierarchy levels, until the packets reach the base station from the bottom level of the hierarchy. Therefore, data packets may pass through multiple nodes to reach the base station. The primary advantage of this topology is the broad area coverage, since the range is not limited to the transmission range of a single node. However, this approach is more complex than the star network and the latency might be increased due to multiple hops from a sensor to the base station. The energy consumption of the network can also be reduced by considering the LoRa physical layer specifications. The proposed algorithm for minimizing the energy consumption of the tree topology is as follows:

- 1) The setting of each node is determined using the proposed algorithm for star networks.

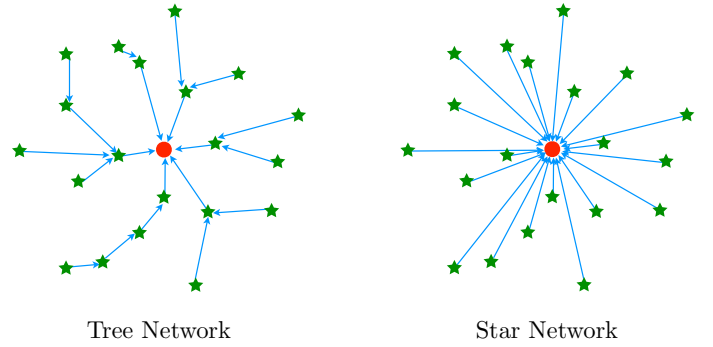


Fig. 1: A sample network with Tree and Star routing topologies.

- 2) The energy consumption of the nodes are calculated based on the transmission power and transmission time using (7).
- 3) The average energy consumption of the network is calculated.
- 4) The data sent from the nodes with energy consumption above the average is re-routed to their nearest node which is closer to the base station. The latter node is called the destination node.
- 5) In the updated network, the destination node receives all such possible data and sends them along with its own data.
- 6) Repeat steps 3-5 for a pre-defined number of iterations (In the experiment conducted by the authors, the iteration is repeated 4 times.)

A sample node placement with both the tree and star network routing topologies is shown in Fig. 1.

## V. ANALYTICAL STUDY

The performance of the LoRa network is influenced by many factors like the location of the nodes, the link quality, and size of the packet. Therefore, the distributed topology is chosen for evaluating the performance of the proposed star and tree LoRa networks. Without loss of generality, It is assumed that the base station is located at  $(0, 0)$  and all  $N$  nodes are uniformly and independently distributed on a circular area defined by  $(r, \varphi)$  points (in the polar coordinates), where  $R_a < r < R_b$ .  $R_b$  is selected according to the LoRa communication range in rural areas and  $R_a$  is a lower-bound to prevent the placement of a node very close to the base-station. Hence, the nodes are scattered in an area of size  $A = \pi(R_b^2 - R_a^2)$ . This implies that the polar coordinate  $(r, \varphi)$  of the nodes are distributed as:

$$r^2 \sim \text{Unif}(R_a^2, R_b^2), \quad \varphi \sim \text{Unif}(0, 2\pi), \quad (9)$$

We further assume that the nodes are stationary and the topology of the network remains unchanged over the time. Let  $\{V_i\}_{i=1}^n$  denote the nodes (no specific order), and let  $\{E_i\}_{i=1}^n$  represent the required energy for a packet to reach the base station from  $V_i$  (which depends on the transmission strategy).

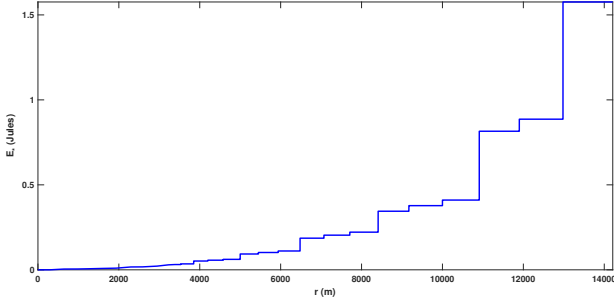


Fig. 2: The optimized energy of the node in terms of the distance of the node to the base station  $r$ .

The average energy consumption of the network when all nodes transmit a single packet is given as:

$$\begin{aligned} \bar{E}_N &= \frac{\mathbb{E}(E_1 + \dots + E_N)}{N} \\ &= \frac{1}{N} \sum_{i=1}^N \mathbb{E}(E_i) = \mathbb{E}(E(r, n)), \end{aligned} \quad (10)$$

where  $E(r, n)$  is the energy required for a packet to reach the base station from a node in distance  $r$  to the base station in the  $n$ -node network. Here, the symmetry of the  $V_i$  in the last equality is used. To further simplify (10), the star and tree are topologies considered separately.

#### A. Star topology

A node can establish a wireless link with the base station if its distance to the base station is less than the LoRa communication range. The probability density function (pdf) of the distance  $r$  between a random node on the disk and the center of the disk is obtained as:

$$p(r) = \begin{cases} \frac{2r}{R_b^2 - R_a^2} & R_a < r < R_b \\ 0 & \text{otherwise} \end{cases} \quad (11)$$

In the star topology, each node is self-configured by applying the proposed algorithm for the star topology. As a result, the energy consumption of the nodes is optimized independently. Evidently, the energy consumption of the node is directly linked with its distance  $r$  to the base station. The optimized energy consumption  $E_{*|r}$  is shown in Fig. 2. Here, the optimization is applied to the spreading factor, the bandwidth, and the transmission power (allowed values by the LoRa standard). Due to the discrete choice of the parameters, the overall graph is piecewise constant with 34 jumps. The average energy consumption of the LoRa star network per packet is given in (12).

$$\bar{E}_{N,star} = \frac{1}{(R_b^2 - R_a^2)} \sum_{i=1}^{34} (r_i^2 - r_{i-1}^2) E_{*|r=(\frac{r_{i-1}+r_i}{2})}, \quad (12)$$

where  $r_0 = R_a$  and  $r_i$  for  $i \geq 1$  is the location of the  $i^{th}$  jump in Fig. 2. To interpret  $\bar{E}_{N,star}$  in a numerical form, we set  $R_a = 500$  m and  $R_b = 14200$  m which are selected according to the LoRa communication range in rural areas. With this choice, the following equations are obtained:

$$\bar{E}_{N,star} = 0.7393 \text{ [Joules]} \quad (13)$$

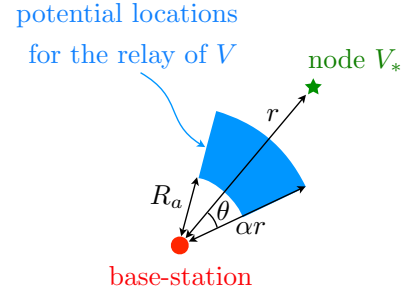


Fig. 3: The geometrical explanation of the parameters  $\alpha$  and  $\theta$ : for each node  $V_*$ , we search for a relay node in a circular section around the base station with central angle  $2\theta$  and radius  $\alpha r$ , where  $r$  is the distance of the node  $V_*$  to the base station.

#### B. Tree topology

In the tree topology, the nodes collaborate in the transmission to avoid a node located far from the base station, transmitting over the long distance. Therefore, we use a routing protocol. To make the analysis simple, we devise the following scheme: we first fix the parameters  $0 < \alpha < 1$  and  $0 < \theta < \pi$ . Then for each node  $V_*$  located at polar coordinate  $(r_*, \varphi_*)$ , we consider the region  $R_a < r < r_*\alpha$  and  $|\varphi - \varphi_*| \leq \theta$ , where  $R_a$  is the lower-bound to prevent the placement of a node very close to the base-station. In words, this region is a circular sector around the base station with central angle  $2\theta$  and maximum radius  $\alpha r_*$  (see Fig. 3). Our strategy is that  $V_*$  sends all its packets to a relay node in this region. More specifically, the relay node for  $V_*$  is the closest node to  $V_*$  in this region; in case this region is empty of nodes, then,  $V_*$  transmits directly to the base station.

As shown in Fig. 4, let  $A_1, O_A, O_B$ , and  $B_1$  be the corner points of the mentioned region ( $R_a < r < r_*\alpha$  and  $|\varphi - \varphi_*| \leq \theta$ ). For illustration of the technique, let the region  $A_1O_AO_BB_1$  (denoted by  $I$ ) be radially divided in to  $k$  narrow rings  $I_1, I_2, \dots, I_k$  ( $k \gg 1$ ). First note that the area of  $I$  is  $\theta((\alpha r_*)^2 - R_a^2)$ ; therefore, the probability that this region is empty of nodes is given by (14) (all  $n-1$  nodes besides  $V_*$  shall fall in the remainder of the disk).

$$\mathbb{P}_{I,e} = \left( 1 - \frac{\theta((\alpha r_*)^2 - R_a^2)}{\pi(R_b^2 - R_a^2)} \right)^{n-1} \quad (14)$$

Thus, with probability  $\mathbb{P}_{I,e}$ , the node  $V_*$  forms a direct link with the base station. Similarly, with probability  $\mathbb{P}_{I,ne} = 1 - \mathbb{P}_{I,e}$ , region  $I$  contains at least one node which shall act as a relay for  $V_*$ .

Now, the energy required for a packet to reach the base station from  $V_*$  is the sum of the energies from  $V_*$  to the relay node and from this relay node to the base station (the relay node might also use other relay nodes). As the relay node is located in one of the  $I_i$ s, we use the upper bound  $|V_*A_i|$  for the distance between  $V_*$  and a relay node in  $I_i$ .

To further proceed, let  $\bar{E}_{(i)}(r)$  be the average energy consumption per packet of a node placed at distance  $r$  from the base station, where the average is over all possible placements

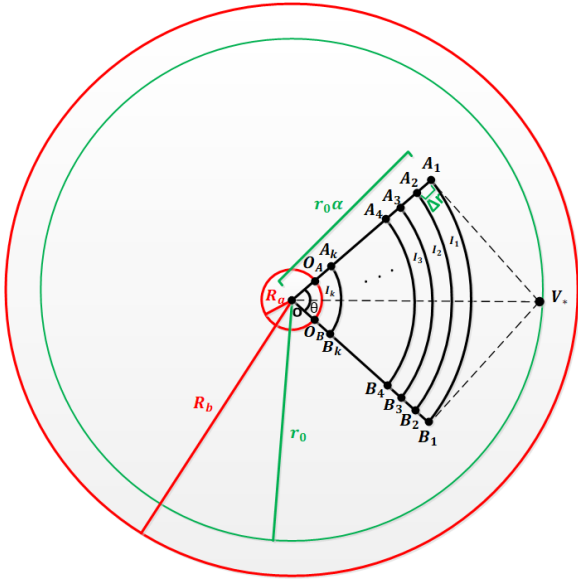


Fig. 4: Simplified model for the tree network analysis.

of the remaining  $i$  nodes (all possible configurations). Below, we first upper-bound  $\bar{E}_{(i)}(r)$ , and then average it over  $r$ :

$$\begin{aligned} \bar{E}_{(n)}(r_*) &\leq \mathbb{P}_{I,e} \times E_{*|r=r_*} + \\ &\sum_{i=1}^k \left[ \mathbb{P}(I_{i,ne} \& I_{1,e} \dots I_{(i-1),e} | I_{ne}) \times \right. \\ &\quad \left. (E_{*|r=|V_*A_i|} + \bar{E}_{(n-1)}(r_i)) \right] \\ |V_*A_i| &= \sqrt{r_*^2 + r_i^2 - 2r_*r_i \cos(\frac{\theta}{2})} \\ r_i &= r_*\alpha - (i-1)\Delta r \end{aligned} \quad (15)$$

The above equation, recursively relates  $\bar{E}_{(i)}(r)$  to itself with smaller values of  $i$  and  $r$ . Let us evaluate the involved probability value:

$$\begin{aligned} \mathbb{P}(I_{i,ne} \& I_{1,e} \dots I_{(i-1),e}) &= \mathbb{P}_{I_{1..i-1}, e} - \mathbb{P}_{I_{1..i}, e} \\ &= f((i-1)\Delta r) - f(i\Delta r), \end{aligned} \quad (16)$$

$$\mathbb{P}(I_{i,ne} \& I_{1,e} \dots I_{(i-1),e} | I_{ne}) = \frac{\mathbb{P}(I_{i,ne} \& I_{1,e} \dots I_{(i-1),e})}{\mathbb{P}_{I,ne}}, \quad (17)$$

where  $f(x) = (1 - \frac{\theta((r_*\alpha)^2 - (r_*\alpha - x)^2)}{\pi(R_b^2 - R_a^2)})^{n-1}$ . Therefore, if we rewrite (15) using (16) and (17), we have:

$$\begin{aligned} \bar{E}_{(n)}(r_*) &\leq \mathbb{P}_{I,e} \times E_{*|r=r_*} + \\ &\frac{1}{1 - \mathbb{P}_{I,e}} \sum_{i=1}^k \left( \frac{f((i-1)\Delta r) - f(i\Delta r)}{\Delta r} \times \right. \\ &\quad \left. [E_{*|r=|V_*A_i|} + \bar{E}_{(n-1)}(r_i)] \times \Delta r \right) \end{aligned} \quad (18)$$

If we let  $\Delta r \rightarrow 0$ , we have that:

$$\begin{aligned} \bar{E}_{(n)}(r_*) &\leq \mathbb{P}_{I,e} \times E_{*|r=r_*} - \\ &\int_{x=0}^{r_*\alpha} f'(x) [E_{*|r=|V_*A_i|_x} + \bar{E}_{(n-1)}(r_*\alpha - x)] dx, \end{aligned} \quad (19)$$

where  $|V_*A_i|_x = \sqrt{r_*^2 + (x - r_*\alpha)^2 + 2r_*(x - r_*\alpha)}$ . Note that  $f(\cdot)$  is decreasing; hence  $f'(x)$  is negative in (19). Due

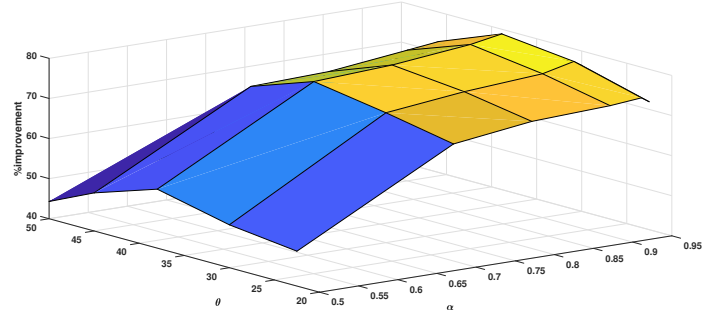


Fig. 5: The improvement percentage of energy consumption of the proposed tree network to star network with 100 nodes in terms of  $\alpha$  and  $\theta$  obtained from (20) and (21).

to the discrete nature of  $E_*$ , we cannot analytically convert (19) into a closed-form upper-bound expression for  $\bar{E}_{(n)}(r_*)$ . However by discretizing the domain, we can numerically evaluate an upper-bound for  $\bar{E}_{(n)}(r_*)$ . We should add that the average energy consumption of the tree topology of LoRa network is given by:

$$\bar{E}_{N,tree} = \int_{R_a}^{R_b} p(r) \times \bar{E}_{(n)}(r) \times dx \quad (20)$$

We can bound this value by plugging in the numerical upper-bound for  $\bar{E}_{(n)}(r)$ .

### C. Performance comparison of the star and tree topologies

The derivation of exact expressions for the energy consumption of the mentioned star and tree topologies is a sophisticated problem. Therefore, the equations are evaluated numerically in MATLAB. In order to compare the total energy consumption of the proposed topologies, the improvement percentage of energy consumption is reported in (21).

$$\%improvement(\alpha, \theta, N) = \frac{(\bar{E}_{N,star} - \bar{E}_{N,tree})}{\bar{E}_{N,star}} \times 100 \quad (21)$$

For a network with 100 nodes, the improvement percentage of energy consumption in terms of  $\alpha$  and  $\theta$ , is depicted in Fig. 5.

According to the numerical results, it can be concluded that by applying the proposed tree algorithm, the total energy consumption of the tree network with 100 nodes can be improved by at least 79.68% ( $\alpha = 0.94$ ,  $\theta = 38^\circ$ ) compared to the star network. As the upper-bound on the energy consumption is considered, the exact value of improvement is expected to be higher (which is confirmed in our following simulation results). We should highlight that, the improvement percentage of energy consumption depends on the total number of nodes. In Fig. 6, we show the dependence of the improvement percentage on the number of nodes. While the inferior performance of the tree topology at small number of nodes ( $N < 10$ ) is observed, it yields no less than 80% improvement when the network scales to ( $N \geq 100$ ).

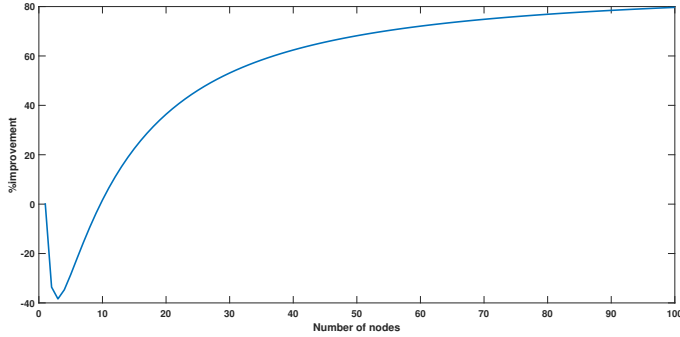


Fig. 6: A lower-bound for the improvement percentage of energy consumption of the proposed tree network to star network with specified configuration ( $\alpha = 0.94$  and  $\theta = 38^\circ$ ) in terms of the size of the network ( $N$ ).

TABLE I: Simulation parameters

Parameter	Value	Description
$P_{TX}$	-2 dBm to 20 dBm	Transmission power
$SF$	6 to 12	Spreading Factor
$BW$	125, 250, and 500	Bandwidth (kHz)
$\gamma$	2.65	Path loss exponent
$X_\sigma$	$\mathcal{N}(0, 3.1)$	Shadowing effect (dB)
$d_0$	1 km	Reference distance
$R$	0.5 km to 14.2 km	Radius of the area
$n_{pm}$	8 bytes	Preamble length
$n_{packet}$	100 bytes	Packet length
Packet interval	60000 s	Mean time between transmission intervals

## VI. SIMULATION RESULTS

The star and tree topologies of LoRa networks are implemented in Python. The simulations are based on LoRa link behaviour described in Section III. The  $N$  nodes are placed randomly and uniformly around the base station. Each node is configured by applying the proposed algorithms and its energy consumption is measured. The simulation parameters are given in Table I.

The improvement percentage of energy consumption of the network with 100 nodes in terms of  $\alpha$  and  $\theta$  is shown in Fig. 7. The simulations are repeated 1000 times for each pair of  $(\alpha, \theta)$  configuration and the average energy improvement is reported. According to the simulation results, it can be concluded that by applying the proposed tree algorithm, the total energy consumption of the network can be reduced by 84.45% ( $\alpha = 0.94, \theta = 45^\circ$ ).

It is interesting that we observe matching  $\alpha_{opt}$  values between our analytical (the upper-bound) and simulation results. The optimum value for  $\theta$  is, however, slightly different; while theory suggests  $38^\circ$ , simulation results indicates  $45^\circ$ . Also as we expected, the exact value of improvement ( $\cong 85\%$ ) is higher than the predicted value based on our analytical results ( $\cong 80\%$ ) using the upper-bound. Note that in our analytical approach, particularity in (15), we evaluate an upper-bound on the average energy consumption by a pessimistic bound

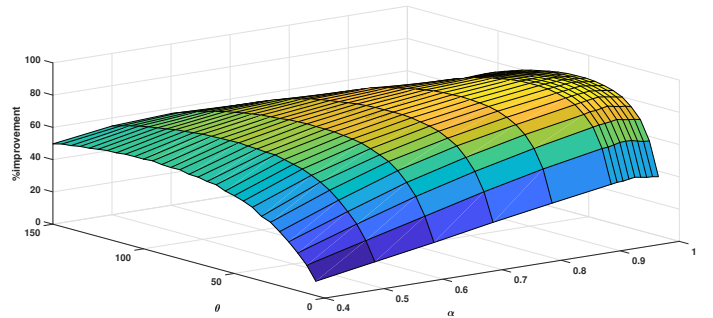


Fig. 7: The improvement percentage of energy consumption of the proposed tree network comparing the star network with 100 nodes in terms of  $\alpha$  and  $\theta$  obtained from simulations.

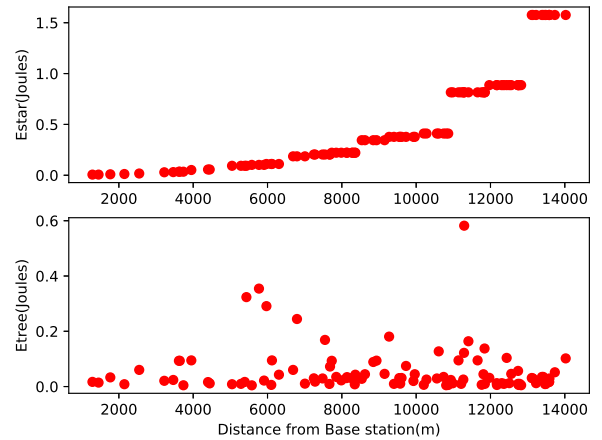


Fig. 8: The energy consumption of the nodes in the star and tree network with 100 nodes with specified configuration ( $\alpha = 0.94$  and  $\theta = 45^\circ$ ) in terms of the distance of the nodes to the base station.

for the distance between a node and its relay.

We have plotted the energy consumption of a typical placement of the 100-node LoRa network for both the star ( $E_{star}$ ) and the tree ( $E_{tree}$ ) topologies in Fig. 8. Besides the overall reduction of the energy consumption in the tree topology, we observe that the energy consumption of the nodes are less varied in the tree topology. Numerically, the standard deviation of  $E_{star}$  and  $E_{tree}$  in this setting are found to be 0.484 [Joules] and 0.0838 [Joules], respectively.

## VII. EXPERIMENTAL RESULTS

To explore the performance of the presented algorithms, the LoRa network with 35 nodes and a base station is set up in an open space of size around  $100^m \times 100^m$ . While the base station is placed in the middle of the field, the location of the nodes are generated randomly via a software simulation. The simulated distances were set similar to a practical scenario which was well beyond the setup area. Therefore, we have scaled down the distances to fit in the available space. Nevertheless, the

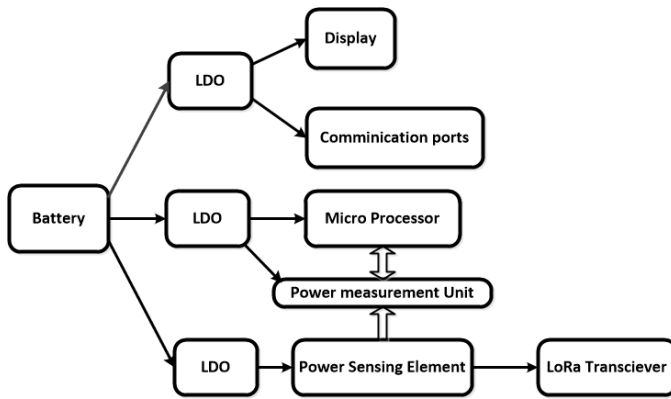


Fig. 9: The block diagram of the power supply section of the experimental setup.

path loss model associated with the original distances were implemented via tunable power attenuation circuits placed ahead of the transmitting antenna of each node (as well as the base station). Each node comprises a Semtech SX1276 LoRa transceiver, a low-power micro-controller (msp430f147), a high dynamic range & high precision power measurement system, a power supply, an RS232 communication port, and a graphic display. The block diagram of the power supply section is shown in Fig. 9. It has three low-dropout (LDO) regulators to maintain a steady power source for all sections of the device, especially, when the battery runs down. The authors have a low-power and low-cost implementation for IoT power measurement that features maximum sampling rate of 5 Mhz, load regulation of 0.16%, and linearity error of 0.32% [37]. The implemented node and network structures are shown in Fig. 10 and Fig. 11, respectively.

In the implemented LoRa network, each node has the ability to send/receive data, measure, and tune its power consumption. The measured powers of the nodes are sent to the central system through LoRa network at specified intervals. The central station has the task of monitoring and controlling the power consumption of the network. It is able to collect the data transmitted by all the nodes within the transmission range. Therefore, the central station can manage and adjust the power consumption of the network by sending the required control commands to the nodes. In our proposed network, the local timing of all nodes is synchronized with the synchronization signal sent by the base station at specified time intervals. Each node has its own specified ID on the network. The specific time slot for receiving and sending data for each node in the network is determined by its ID. The ID setting in our current setup is static but can be determined dynamically in the future. The size of the synchronization packets, the routing information, and the transmission time intervals are set in a way that the nodes and the base station follow the 1% duty cycle constraint. For a better overview of the routing procedure, we provide a summary here:

- Each node sends a packet containing its ID at its specified time slot to the network, and all other nodes listen to the channel. All other nodes in the listening mode receive and archive the transmitted packets.



Fig. 10: The implemented node consists of a power measurement unit, a power supply, a processor, LoRa transceiver, and an RS232 communication port.

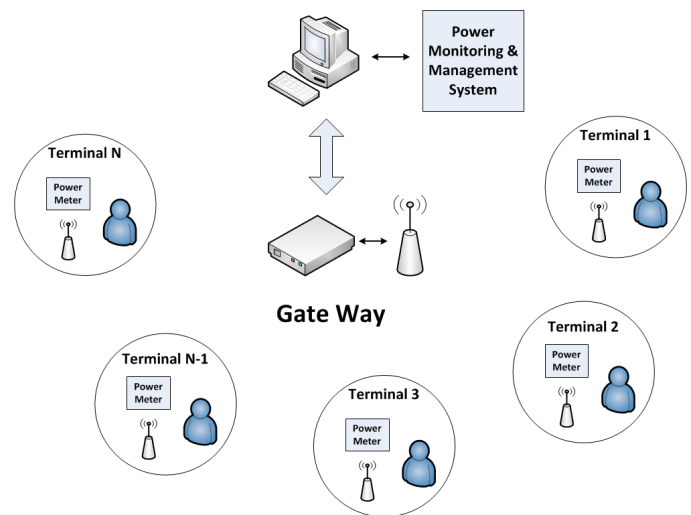


Fig. 11: The implemented LoRa network.

- The previous step is repeated for a pre-defined number of iterations which depends on the number and distribution of the nodes in the network (in the experiment conducted by the authors, 5 iterations are used).
- Each node sends a packet containing its own ID and the list of its received signal strength indicators (RSSI) from other nodes (each RSSI is also accompanied with the ID of the associated node).
- The base station schedules the network based on the received packets from the nodes and their RSSI values.
- The base station broadcasts the determined routing path and configuration of the nodes to the network.

The experiment is repeated for 20 different random placements of the nodes and the average energy consumption of the star and tree topologies are measured. The measured improvement percentage of energy consumption of the tree network with 35 nodes compared to the star network is 46%. The analytical and simulation results indicate that the energy consumption of the network with 35 nodes can be improved

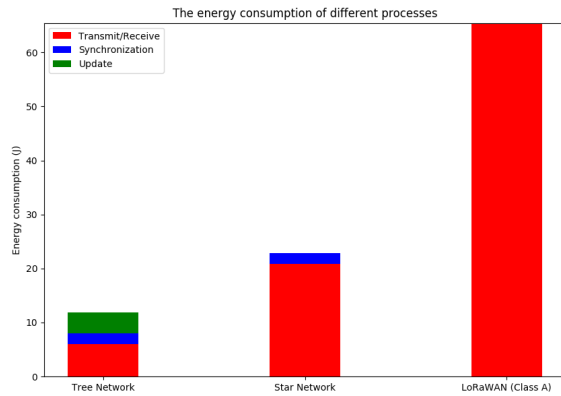


Fig. 12: The energy consumption of different processes of LoRAWAN, the star, and the tree networks with 35 nodes.

by 58.36% and 69.26%, respectively. The energy improvement measured from the experimental platform is less than both the simulation and analytical results because the energy consumed for the synchronization process, distribution/updating the routing information, and receiving the data by the nodes are ignored in simulation and analytical studies. It should be noted that according to the static nature of the network, the routing is done in the beginning and is not updated very frequently. The average energy consumption of different processes of LoRAWAN (with ADR-enabled class A nodes having lowest energy consumption), the star, and the tree network with 35 nodes for 30 cycles is reported in Fig. 12.

## VIII. CONCLUSIONS

This paper proposed a tree-based routing algorithm for LoRa networks to achieve a more energy-efficient network. Contrary to the conventional star-based LoRa network, the nodes can act as relays to propagate the data from nodes farther from the base station. The physical layer configuration and routing of the nodes are determined by the proposed algorithms. The performance and efficiency of the algorithms are verified through analytical calculations, simulations, and practical experiments. The analytical and simulation results indicate that the energy consumption of the LoRa network with 100 nodes in the tree topology is around 80% below that of the star topology. Moreover, the performance of the proposed topology depends on the number of the nodes and reduces by scaling down the number of the nodes. For instance, the improvement percentage of energy consumption of the tree network with 35 nodes obtained from analytical, simulation, and experimental results is around 58%, 69%, and 46%, respectively. The energy improvement measured in the experimental platform is less than both simulation and analytical results, because the reception energy consumption was ignored in our simulations and theoretical studies. In the star network, the farther the node is located from the base station, the higher energy consumption is required. Therefore, the battery lives of the farther nodes from the base station are reduced. This in term causes the network imbalance and calls

for more services and considerations. One of the advantages of the tree-topology is that the consumed energy across the nodes becomes more uniform. The main focus of this paper is to investigate the energy efficiency of the proposed tree-based LoRa network. However, the network coverage, throughput, and interference issues are likely to be improved which should be studied in future researches.

## REFERENCES

- [1] W. Ayoub, A. E. Samhat, F. Nouvel, M. Mroue, and J.-C. Prévotet, "Internet of mobile things: Overview of LoRaWAN, DASH7, and NB-IoT in lpwans standards and supported mobility," *IEEE Communications Surveys & Tutorials*, vol. 21, no. 2, pp. 1561–1581, 2018.
- [2] Y. H. Tehrani, Z. Fazel, and S. M. Atarodi, "A survey of two dominant low power and long range communication technologies," *Journal of Information Systems Telecommunications*, vol. 6, no. 22, 2018.
- [3] A. Augustin, J. Yi, T. Clausen, and W. Townsley, "A study of LoRa: Long range & low power networks for the internet of things," *Sensors*, vol. 16, no. 9, p. 1466, 2016.
- [4] Semtech, "Lora modulation basics, AN1200. 22, revision 2," 2015.
- [5] G. Zhu, C.-H. Liao, M. Suzuki, Y. Nurusue, and H. Morikawa, "Evaluation of lora receiver performance under co-technology interference," in *2018 15th IEEE Annual Consumer Communications & Networking Conference (CCNC)*, pp. 1–7, IEEE, 2018.
- [6] A. Mahmood, E. Sisinni, L. Guntupalli, R. Rondón, S. A. Hassan, and M. Gidlund, "Scalability analysis of a LoRa network under imperfect orthogonality," *IEEE Transactions on Industrial Informatics*, vol. 15, no. 3, pp. 1425–1436, 2018.
- [7] N. Sornin, M. Luis, T. Eirich, T. Kramp, and O. Hersent, "LoRa specification 1.0 LoRa alliance standard specification," *LoRa Alliance*, p. 87, 2015.
- [8] M. Slabicki, G. Premsankar, and M. Di Francesco, "Adaptive configuration of LoRa networks for dense IoT deployments," in *NOMS 2018-2018 IEEE/IFIP Network Operations and Management Symposium*, pp. 1–9, IEEE, 2018.
- [9] L. Casals, B. Mir, R. Vidal, and C. Gomez, "Modeling the energy performance of LoRaWAN," *Sensors*, vol. 17, no. 10, p. 2364, 2017.
- [10] R. Soua and P. Minet, "A survey on energy efficient techniques in wireless sensor networks," in *2011 4th Joint IFIP Wireless and Mobile Networking Conference (WMNC 2011)*, pp. 1–9, IEEE, 2011.
- [11] O. Younis and S. Fahmy, "Heed: a hybrid, energy-efficient, distributed clustering approach for ad hoc sensor networks," *IEEE Transactions on mobile computing*, vol. 3, no. 4, pp. 366–379, 2004.
- [12] D. Kumar and R. Patel, "Multi-hop data communication algorithm for clustered wireless sensor networks," *International Journal of Distributed Sensor Networks*, vol. 7, no. 1, p. 984795, 2011.
- [13] X. Xia, Z. Chen, D. Li, and W. Li, "Proposal for efficient routing protocol for wireless sensor network in coal mine goaf," *Wireless personal communications*, vol. 77, no. 3, pp. 1699–1711, 2014.
- [14] C. Perkins, E. Belding-Royer, and S. Das, "RFC3561: Ad hoc on-demand distance vector (AODV) routing," 2003.
- [15] T. Clausen and P. Jacquet, "RFC3626: Optimized link state routing protocol (OLSR)," 2003.
- [16] C. E. Perkins and P. Bhagwat, "Highly dynamic destination-sequenced distance-vector routing (DSDV) for mobile computers," *ACM SIGCOMM computer communication review*, vol. 24, no. 4, pp. 234–244, 1994.
- [17] D. Johnson, Y.-c. Hu, D. Maltz, *et al.*, "The dynamic source routing protocol (DSR) for mobile ad hoc networks for IPv4," tech. rep., RFC 4728, 2007.
- [18] Z. Haas, "The zone routing protocol (ZRP) for ad hoc networks," *IETF Internet draft, draft-ietf-manet-zone-zrp-01.txt*, 1998.
- [19] F. Adalanto, X. Vilajosana, P. Tuset-Peiro, B. Martinez, J. Melia-Segui, and T. Watteyne, "Understanding the limits of LoRaWAN," *IEEE Communications magazine*, vol. 55, no. 9, pp. 34–40, 2017.
- [20] O. Georgiou and U. Raza, "Low power wide area network analysis: Can LoRa scale?," *IEEE Wireless Communications Letters*, vol. 6, no. 2, pp. 162–165, 2017.
- [21] Semtech, "Sx1276/77/78/79 datasheet." <http://www.semtech.com/images/datasheet/sx1276.pdf>, 2017. Accessed on 2020-3-3.
- [22] D. Croce, M. Gucciardo, S. Mangione, G. Santaromita, and I. Tinnirello, "Impact of LoRa imperfect orthogonality: Analysis of link-level performance," *IEEE Communications Letters*, vol. 22, no. 4, pp. 796–799, 2018.

- [23] L. Vangelista, "Frequency shift chirp modulation: The LoRa modulation," *IEEE Signal Processing Letters*, vol. 24, no. 12, pp. 1818–1821, 2017.
- [24] LoRa Alliance, *LoRaWAN 1.1 Regional Parameters technical specification*, 2017.
- [25] R. S. Sinha, Y. Wei, and S.-H. Hwang, "A survey on LPWA technology: LoRa and NB-IoT," *Ict Express*, vol. 3, no. 1, pp. 14–21, 2017.
- [26] LoRa Alliance, *LoRaWAN specification*, 2015.
- [27] M. C. Bor, U. Roedig, T. Voigt, and J. M. Alonso, "Do LoRa low-power wide-area networks scale?," in *Proceedings of the 19th ACM International Conference on Modeling, Analysis and Simulation of Wireless and Mobile Systems*, pp. 59–67, ACM, 2016.
- [28] G. Callebaut and L. Van der Perre, "Characterization of LoRa point-to-point path-loss: Measurement campaigns and modeling considering censored data," *IEEE Internet of Things Journal*, Early Access, 2019.
- [29] M. Viswanathan, "Log distance path loss or log normal shadowing model," 2013, Accessed July 3, 2020. <http://www.gaussianwaves.com/2013/09/log-distance-path-loss-or-log-normal-shadowing-model/>.
- [30] J. Goldhirsh and W. J. Vogel, "Handbook of propagation effects for vehicular and personal mobile satellite systems," *NASA Reference Publication*, vol. 1274, pp. 40–67, 1998.
- [31] B. Sartori, S. Thielemans, M. Bezunartea, A. Braeken, and K. Steenhaut, "Enabling RPL multihop communications based on LoRa," in *2017 IEEE 13th International Conference on Wireless and Mobile Computing, Networking and Communications (WiMob)*, pp. 1–8, IEEE, 2017.
- [32] C.-H. Liao, G. Zhu, D. Kuwabara, M. Suzuki, and H. Morikawa, "Multi-hop LoRa networks enabled by concurrent transmission," *IEEE Access*, vol. 5, pp. 21430–21446, 2017.
- [33] *LoRa for the Internet of Things*, International Conference on Embedded Wireless Systems and Networks, 2016.
- [34] H.-C. Lee and K.-H. Ke, "Monitoring of large-area IoT sensors using a LoRa wireless mesh network system: Design and evaluation," *IEEE Transactions on Instrumentation and Measurement*, vol. 67, no. 9, pp. 2177–2187, 2018.
- [35] N. C. Almeida, R. P. Rolle, E. P. Godoy, P. Ferrari, and E. Sisinni, "Proposal of a Hybrid LoRa Mesh/LoRaWAN network," in *2020 IEEE International Workshop on Metrology for Industry 4.0 & IoT*, pp. 702–707, IEEE, 2020.
- [36] M. S. Aslam, A. Khan, A. Atif, S. A. Hassan, A. Mahmood, H. K. Qureshi, and M. Gidlund, "Exploring Multi-Hop LoRa for green smart cities," *IEEE Network*, vol. 34, no. 2, pp. 225–231, 2019.
- [37] Y. H. Tehrani and S. M. Atarodi, "Design & implementation of a high precision & high dynamic range power consumption measurement system for smart energy iot applications," *Measurement*, vol. 146, pp. 458–466, 2019.